

Anomalies and cycles of precipitable water over Iran in recent decades

Hossein Asakereh¹ · Mehdi Doostkamian¹ · Sahar Sadrafshary¹

Received: 27 November 2014 / Accepted: 16 March 2015 / Published online: 9 April 2015
© Saudi Society for Geosciences 2015

Abstract Water vapor transported by atmospheric circulation is an important aspect of the hydrologic cycle and plays a vital role in determining rainfall distribution. Much effort has been devoted to investigation of anomalies and cycles of precipitable water over Iran using air pressure and specific humidity data (1981–2010) from the National Center for Environmental Prediction and the National Center for Atmospheric Research. The results of the present study indicate that the coastal areas experienced positive anomalies owing to their proximity to large bodies of water, while upland areas and the northwest and northeast of the country experienced negative anomalies because of their distance from water resources and altitude. The results of cycle analysis revealed that short cycles (i.e., 2- to 5-year cycles) occurred in most of the country. The shortest cycles occurred in the southeast region. Scientists are in agreement that the 2- and 5-year cycles are related to the El Niño southern oscillation and quasi-biennial oscillation in the general circulation of the atmosphere.

Keywords Perceptible water · Anomalies · Cycle analysis · Iran

Introduction

Atmospheric water vapor is a principal contributor to the greenhouse effect and plays a key role in understanding the earth's climate (Ernest et al. 2008; Hadjimitsis et al. 2011), long-term changes in water vapor, the annual cycle of atmospheric moisture, and related processes (Gaffen et al. 1992). Precipitable water is an important factor affecting precipitation. Its behavior is studied by climatologists for short- and long-term climate change. Some scientists have deployed numerical models of weather and climate to investigate the variability of precipitable water (Surcel et al. 2010; Vasic et al. 2007). Improvements in radar and remote sensing satellites (Nesbitt and Zipser 2003; Biasutti et al. 2011) and the availability of reanalyzed data (Kalnay et al. 1996) have made access to reanalyzed data on a global scale for the study of precipitable water more feasible.

Investigating the decadal changes in precipitable water is essential for understanding local and regional climate change. Identifying these decadal changes can aid detection of variations of this element and can be used for environmental planning based on precipitation. Precipitable water is a climatic element that shows tempo-spatial variation. Solar heating near the surface and in the adjacent atmosphere generates strong diurnal oscillations in the surface and atmospheric temperature which affects pressure patterns and determines wind fields. These changes lead to anomalies at given points and for all points at the same latitude. These oscillations, in turn, can cause oscillations in the precipitable water in the atmosphere.

Carl et al. (2007) examined affirmation feedback, and the relationship between changes in temperature and changes in precipitable water using station databases, climate model data, and reanalyzed data sets. They found that these variables were highly correlated, particularly over tropical oceans. Tingley

✉ Hossein Asakereh
asakereh@znu.ac.ir

¹ University of Zanjan, Zanjan, Iran

(2012) maintains that surface anomalies are caused by stochastic climate events, but some occur in regular patterns; for instance, mid-latitude positive anomalies could occur in response to anomalies in oceanic currents or from El Niño southern oscillation (ENSO) (Tingley 2012). Accordingly, the increase in temperature at the end of the last century could lead to changes in the hydrological cycle (Azizi and Roshani 2008).

Spatial and temporal variations in climate elements are evident in Iran because of the complexity of its topography (Asakereh 2007; Ghaiur and Masudian 1996). Asakereh (2007) categorized these variations into oscillation and fluctuation forms. Tempo-spatial variation could also have occurred in precipitable water over Iran. Understanding these cycles is of paramount importance, particularly in areas with complex topography, for development of climate prediction models and accurate reproduction of the cycles (Yang and Slinger 2001; Lee et al. 2007).

Harmonic analysis is one method for analysis of the temporal behavior of climatic patterns (Rouault et al. 2012). Harmonic analysis explains time-series fluctuations in terms of sinusoidal behavior at different frequencies and considers the different frequencies and wavelengths in a time-series (Asakereh and Razmi 2012). Experts in the field (e.g., Chen et al. 1996; Collier and Bowman 2004; Kniviel et al. 2004) have studied the cycles in relation to large- and small-scale circulation using harmonic analysis. This method has been employed primarily to investigate regional, local, seasonal, and annual precipitation scales (Wallace 1975; Twardosz 2007) and marine (Carbone and Tuttle 2008) and continental studies (Kerns et al. 2010).

Sen-Roy and Balling (2005) used harmonic analysis and concluded that the daily precipitation cycles in Puerto Rico were related to the Katabatic and Anabatic daily patterns that interact with easterly winds and are less affected by the southern oscillations. Kalaycı et al. (2004) used harmonic analysis to investigate the monthly and annual characteristics of precipitation at 50 stations in Europe. Hartmann et al. (2008) discovered biennial periods in precipitation time series of China using harmonic and autocorrelation analysis and relating them to quasi-biennial oscillation (QBO). The present study used harmonic analysis to examine the complex topography of Iran and reveal the cycles for precipitable water.

Location and typography of Iran

Iran is located in southwest Asia. It features high mountains on four sides and borders with seas to the south and north (Fig. 1). This location creates intra-annual variations in temperature and the occurrence of spatial differences. The large area of the country (approximately 1,600,000 km²), its wide latitudinal extent (25 to 40 N), and its pronounced relief

contribute to the complex structure of humidity distribution over Iran.

The wide latitudinal extent of Iran places it in many system paths that can produce humidity in a tempo-spatial fashion. Under given conditions, the systems causing the different levels of humidity each operate in different spaces and time scales. These systems come from outside the country (e.g., Siberia, Arabian Peninsula) and from inside (high mountains ranges) (Alijani 1994). The two highest mountain ranges are the Zagros and Alborz-Talish, which reach 4557 and 5670 m in elevation, respectively (Fig. 1b), and strongly affect the temporal and spatial patterns of humidity. The Zagros Mountains in western Iran runs northwest to southeast; the northern Alborz-Talish range runs west to east along southern coast of the Caspian Sea.

Data and method

To describe the anomalies and annual precipitable water cycle over Iran, the gridded daily data for pressure and humidity were obtained from the National Center for Environmental Prediction and the National Center for Atmospheric Research (Kalnay et al. 1996). The data set consists of grid-point values of 2.5°×2.5° for the years 1950–2010. Doty (1995) used GrADS software to calculate the sum of the humidity mass-weighted layers for surface pressure (1000 hPa on the bottom) and at 275 hPa as follows:

$$PW = \frac{1}{g} \int_{1000}^{275} q dp \quad (1)$$

where g is acceleration of the earth gravity, q is specific humidity (g/g), and p is pressure. The result is g/m² of water or, essentially, precipitable water (PW; mm). A set of PW time series was created for each 2.5°×2.5° pixel for the period 1950–2010. The annual PW values were calculated for the following stages:

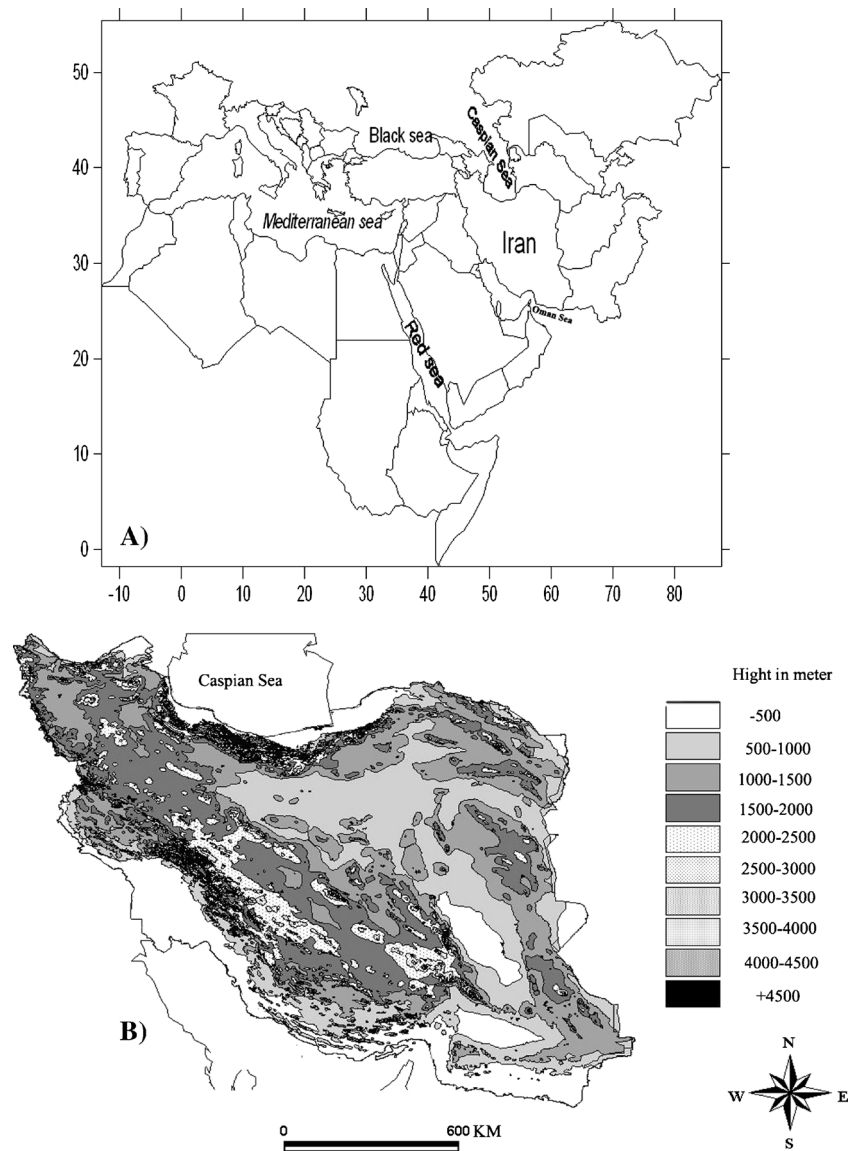
1. The spatial PW mean of each decade (PW_{*i,j*}) was calculated to examine the decadal variation in the spatial PW mean as:

$$PW_{i,j} = \frac{\sum_j \sum_i PW_{i,j}}{n} \quad (2)$$

To detect the way in which fluctuations occur, PW anomalies were compared to each mean of the long-term pixels for each decade (PW_{mean,*j*}) as:

$$PW_{\text{Anomaly}} = PW - PW_{\text{mean},j} \quad (3)$$

Fig. 1 Iran: **a** geographic location in southwest Asia; **b** topographical features



The anomaly maps were obtained using the difference between the annual mean maps for each decade and the total mean precipitable water of the entire study period.

2. As stated, some climatic variation occurs as oscillatory behavior; although many sets of data might not appear to be periodic, they contain interesting periodic components. Bloomfield (2000) stated that harmonic analysis is invaluable for detecting such components. Harmonic analysis, thus, was performed on annual PW to estimate its cyclic behavior. A number of harmonic functions with different frequency amplitudes and phases were constructed on each pixel in the PW time series. In this method, the variance distribution along the entire wavelength of the time series was presented, and the

time series were converted to frequency functions. Determining the effective parameters in the variance of frequency is the objective of harmonic analysis; therefore, successive waves in a periodic time series are shown using a harmonic analyzer (Ghaiur and Asakereh 2005). Niroumad and Bozorgnia (2002) extracted cycles through a harmonic analyzer by first calculating the Fourier coefficients using the following formula:

$$\begin{aligned}
 a_l &= \frac{2}{n} \sum_{t=1}^n PW_t \cos\left(\frac{2\pi l}{n} t\right) & l = 1, 2, \dots, \frac{n}{2} \\
 b_l &= \frac{2}{n} \sum_{t=1}^n PW_t \sin\left(\frac{2\pi l}{n} t\right) & l = 1, 2, \dots, \frac{n}{2}
 \end{aligned}
 \tag{4}$$

where l is the number of harmonics ($l=n/2$ for even and $l=(n-1)/2$ for odd lengths). The variance of each frequency is obtained as follows (Nesbitt and Zipser 2003):

$$I(f_i) = \frac{n}{2} (a_i^2 + b_i^2) \quad (5)$$

Significance was determined using variance mean of frequencies (\bar{s}) and first-order autocorrelation of the data (r_1) as follows (Mitchell et al. 1966):

$$\lambda_i = \bar{s} \left[\frac{1-r_1^2}{1+r_1^2-2r_1 \cos\left(\frac{\pi i}{l}\right)} \right] \quad (6)$$

Chi-square testing was used to define the confidence intervals (generally 95 %) and significance of cycles as follows:

$$\lambda_i \frac{\chi_v^2(0.95)}{\nu} \leq \hat{I}(f) \leq \lambda_i \frac{\chi_v^2(0.05)}{\nu} \quad (7)$$

Numerous cycles were spotted in each pixel. Hierarchical cluster analysis was applied to the cycle data set using the squared Euclidian distance and Ward's algorithm for cluster fusion, and a pigeonhole cycle was detected.

Discussion and results

Anomalies

Figure 1 shows the spatial distribution of precipitable water, the anomalies and mean center for three decades (1981–1990, 1991–2000, 2001–2010), and for the entire period under study (1981–2010) over Iran.

Despite the distance from water bodies, the mean precipitable water was higher in central Iran than in the Zagros highlands. This increase in mean precipitable water in central Iran may be the result of increased temperature in the center of the country in response to the increase in water vapor in the atmosphere. The highest average precipitable water occurred on the first decade at 15.1 mm (Table 1). Throughout the study period, the lowest average precipitable water was recorded for the highlands (Table 1).

Figure 1 shows the positive (PA) and negative (NA) anomalies in dark and light colors, respectively, to indicate increases and decreases in precipitable water. Table 1 shows the percentages of areas having positive and negative anomalies. Throughout the study period, 25 % of the country experienced positive anomalies, particularly along the coasts, and 75 % of the country experienced negative anomalies, particularly the mountains and inland areas in the center, east, northwest, and northeast of the country (Table 1 and Fig. 1).

Positive anomalies were detected in all areas along the northern and southern coasts in all decades and for total averages. Recent surveys indicate that the humidity rate is high over bodies of water and near the seas and is low in the Arctic and at high latitudes on monthly and annual scales (Stanton 1968; Parameswaran and Krishnamurthy 1990; Alijani 1994; Hadjimitsis et al. 2011). Mountains and inland deserts in Iran experienced negative anomalies during all periods. Alijani (1994) maintains that this could be the result of low humidity in the mountains and inland deserts. Asakereh and Doostkamian (2014) suggest that the low values of precipitable water over the mountains and inland areas of Iran could be the result of decreases in wet advection in the country in recent decades. It is important to know that an increase in altitude increases the distance from water bodies and decreases the atmospheric temperature and moisture. Moreover, the decrease in atmosphere results in negative anomalies for precipitable water (Fig. 2).

Table 1 and in Fig. 2 show that the areas with negative anomalies have gradually increased since the first decade of the study. In the first decade, approximately 66.7 % of the country experienced negative anomalies; in the last decade, 26.7 % of the country experienced positive anomalies. This difference could be the result of the increase in temperature over the country in the last century. These findings are in line with the findings of Montazeri (2014), who employed the linear regression (LR) and Mann-Kendall (MK) methods. They found that the temperature in Iran has increased in recent decades, particularly in flat and low elevation areas. In these areas, 60 % of the country experienced an increase in minimum temperature, and about 27 % of the country experienced an increase in maximum temperature. The results of the present study confirm these findings.

Table 1 Area covered (%) by positive and negative precipitable water anomalies

Annual anomalies	First decade (1981–1990)	Second decade (1991–2000)	Third decade (2001–2010)	All Periods (1981–2010)
NA (%)	66.7	68.5	73.3	75
PA (%)	33.30	31.50	26.7	25
Spatial mean (mm)	14.8	13.7	13.6	14.2
Spatial CV (%)	26.36	27.2	28.4	27.1

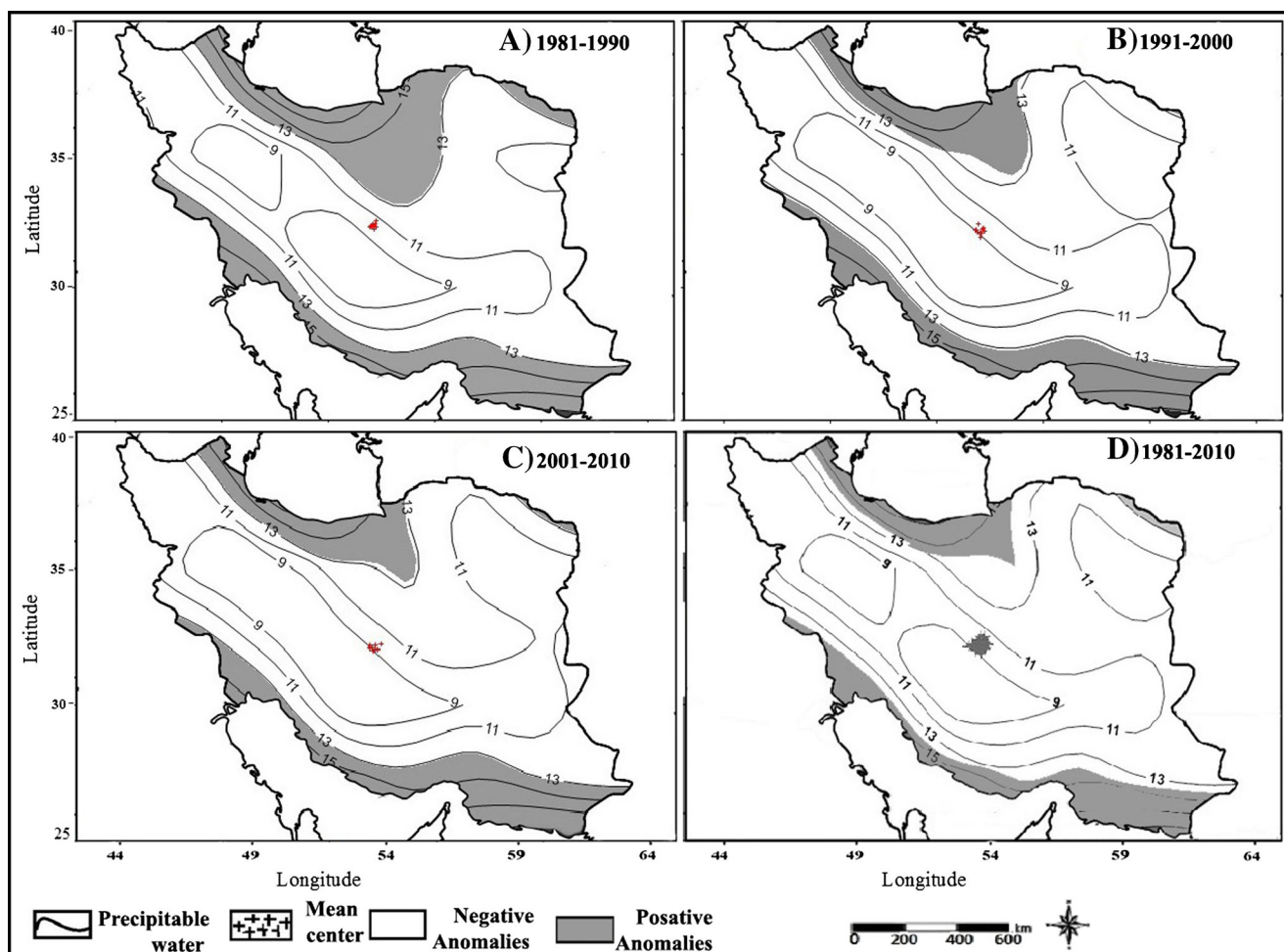


Fig. 2 Spatial distribution of precipitable water, anomalies and mean center for three successive decades (a–c) and entire period under study (d)

In the second decade (1991–2000), 37.5 % of the country showed high positive anomalies. This might have been a result of the cyclic behavior found by Asakreh (2009) in one station in northwest Iran. During this decade (1991–2000), a decrease in the area experiencing positive anomalies coincided with a decrease in the decadal mean of precipitable water, as shown in the third row of Table 1.

The mean center was plotted for the entire period under study for all decades (Fig. 1) and is denoted by (+) on the maps. As seen, the mean center inclined to the south (southern coasts), indicating the greater role of precipitable water in the southern coastal areas compared to the northern coast. Some experts (e.g., Carvalho et al. 2007) believe that the climate anomalies are primarily caused by atmospheric processes in the tropics, mid-latitudes, and subtropical high-pressure regions that interact with oceanic currents. The increase in positive anomalies in the adjacent open seas (Oman Sea) could have a significant effect on spatial mean. The increase in the coefficients of variation (CV) shown in the fourth row of Table 1 confirms these findings.

Annual cycles

Significant sinusoidal cycles were detected by harmonic analysis applied to the data set. Figure 3 shows the cycles classes detected. In northeastern Iran, 2- through 5-year cycles were detected. In southeastern Iran, 2- through 8-year cycles were detected. In the northwest, 2-, 3-, 6-, and 11-year cycles were detected. In the southwest 2-, 3-, and 16-year cycles were detected. Inter-annual variability (2–5 years) is evident across wide areas. This suggests that precipitable water cycles were shorter in many parts of the country. The shorter cycles were more frequent in the southeast in which 2- through 8-year cycles were detected.

Lana et al. (2005) detected 4.6- and 2.1-year cycles in northeastern Spain and attributed them to the QBO. He attributed 9.2- and 5.5-year cycles to the NAO. QBO can be attributed to significant cycles, such as those in southeast (Ghaiuri and Khosravi 2002) and northwest (Asakereh and Razmi 2012) Iran which mainly experience summer rainfall. Azad et al. (2009) concluded that the 3- to 5-year cycles in Indian monsoon precipitation were caused by ENSO. It was observed

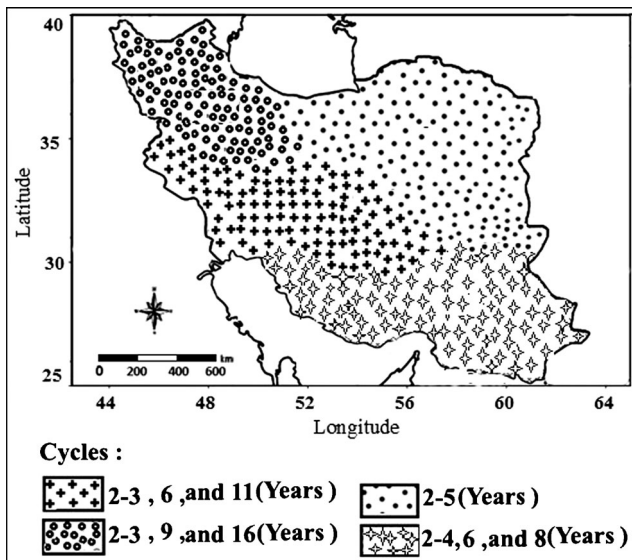


Fig 3 Spatial distribution of annual precipitable water cycles over Iran

that 72.4 % of the region was affected by 2- to 4-year cycles and that 6- and 8-year cycles covered less than 25 % of the region (Table 2).

The largest and the most diverse cycling occurred in the Zagros Mountains, parts of the southwest and in the central parts of the country. In these areas, in addition to the 2-, 3-, and 6-year cycles, longer cycles of up to 11 years also occurred. Jahanbakhsh and Edalatdust (2008) concluded that cycles of sunspot activity and the NAO caused the 11-year cycles in the climate of the country; however, less than 2 % of the region was affected by the 11-year cycles. The most varied cycles correlated with the most intense negative anomalies.

Variability in the cycles could be the result of changes in the precipitation patterns. Weihong et al. (2007) studied the variation in cycles in China and believed them to be linked with changes in the southern monsoon currents of the eastern and western currents in northwest China. They assert that diversity and changes in rainfall patterns caused flooding in one area and drought in another area. It can be concluded that, in addition to the large-scale atmospheric circulation and systems, local factors and neighboring effects were also

involved in precipitable water patterns of the country. Factors such as proximity to water bodies in the south and north of Iran, roughness in the Zagros Mountains and inland deserts can create great variety in precipitable water patterns. Pritchard and Somerville (2009) stated that the variability in precipitation cycles in the southeastern USA was caused by Atlantic currents. The 2- to 4-year cycles were more evident in the northwest of the country.

Precipitable water cycles varied in northwestern Iran, such as in the Zagros Mountains and parts of the southwest, where 2- and 3-year cycles occurred more frequently in 69.2 % of the country (Table 2). Scientists have attributed 2- to 4-year cycles to the ENSO and QBO, large-scale general circulation patterns and climatic and oceanic processes (Garcia et al. 2002; Hartmann et al. 2008).

In the northeast and some parts of central Iran, 2- to 5-year cycles were also observed. These have been attributed to El Niño. Kalaycı et al. (2004) linked 2- to 5-year cycles of precipitation in Turkey to El Niño. More than 31 % of the country (northeastern and parts of central Iran) experienced 2- to 5-year cycles. Other cycles for the same study period were observed in most parts of Iran, except the southeast, and were found to be related to trends found in the data. The cycles in the northwest covered 6.6 % of the total area of this district, which coincides with 32.2 % of the country (Table 2).

Conclusion

Global warming caused by the increase in greenhouse gases is undeniable. The parts of the environment where most biological processes occur are affected by climate change and its abnormalities. Evaluating the precipitable water cycle and anomalies is essential to understanding this interaction. Such studies can help communities prepare for the detrimental effects of climate change and decrease losses caused by changes in the hydrological cycle. The present study employed pressure and humidity data for 1981–2010 to estimate precipitable water in the atmosphere of Iran. Positive anomalies were detected in the coastal areas for the three periods studied and

Table 2 Area over Iran (%) covered by precipitable water cycles from 1950 to 2010

Group 1		Group 2			Group 3			Group 4			
Cycles (year)	Area coverage (%) of		Cycles (year)	Area coverage (%) of		Cycle (year)	Area coverage (%) of		Cycle (year)	Area coverage (%) of	
	Group	The country	Group	Group	The country	Group	Group	The country	Group	Group	The country
2–5	90.1	31.4	2–4	72.4	12.2	2–3	80.9	29.6	2–3	69.2	8.1
24	3.3	1.1	6	13.7	3.3	6	3.1	1.1	9	5.2	0.58
			8	10.3	1.7	11	1.5	0.58	16	5.2	0.58

negative anomalies were found in central Iran because of its remoteness from sources of humidity and increased elevation.

The results indicate that 2- to 5-year cycles dominate the country. Most scientists have attributed the 2- to 4-year cycles to the ENSO and QBO, large-scale general circulation patterns, and climatic and oceanic processes. The most varied cycles (2-, 3-, 6-, 9-, and 1-year) occurred in the south and southwest of the country that are bordered by the Zagros Mountains on one side and water bodies on the other. The most intense negative anomalies occurred in these regions. Moreover, like in the southwest, different cycles have been observed in the northwest of the country from the effect of large mountains, like Sahand and Sabalan.

References

- Aljani B (1994) Climate of Iran. Payam Noor University Press, Tehran
- Asakereh H (2007) Tempo-spatial changes of Iran precipitation during recent decades. *J Geogr Dev* 10:145–164
- Asakereh H, Doostkamian M (2014) Tempo-spatial changes of perceptible water in the atmosphere of Iran. *Iran-Water Resour Res* 10:72–86
- Asakereh H, Razmi R (2012) Analysis of the annual precipitation changes in northwest of Iran. *Geogr Plann* 3:147–162
- Asakereh H (2009) Harmonic analysis of the annual temperature time series of Tabriz. *Q Geogr Res* 93:33–50
- Azad S, Vigneshb TS, Narasimha R (2009) Periodicities in Indian monsoon rainfall over spectrally homogeneous regions. *Int J Climatol* 30:2289–2298
- Azizi G, Roshani M (2008) Studying the climate change on southern shores of the Caspian Sea by using Mann-Kendall test. *Phys Geogr Res* 63:13–28
- Biasutti M, Yuter SE, Burleyson CD, Sobel AD (2011) Very high resolution rainfall patterns measured by TRMM precipitation radar: seasonal and diurnal cycles. *Clim Dyn* 39:239–258
- Bloomfield P (2000) Fourier analysis of time series; an introduction, 2nd edn. Wiley, U.S.A., p 3
- Carbone RE, Tuttle JD (2008) Rainfall occurrence in the U.S. warm season: the diurnal cycle. *J Clim* 21:4132–4146
- Carl AM, Benjamin DS, Frank JW, Karl ET, Michael FW (2007) Relationship between temperature and precipitable water changes over tropical oceans. *Geophys Res Lett* 34:101–120
- Carvalho AA, Tonis C, Jones H, Rocha R, Polito PS (2007) Antipersistence in the global temperature anomaly field. *Nonlin. Process Geophys* 14:723–733
- Chen M, Dickinson RE, Zeng X, Hahmann AN (1996) Comparison of precipitation observed over the continental United States to that simulated by a climate model. *J Climate* 9:2233–2249
- Collier JC, Bowma KP (2004) Diurnal cycle of tropical precipitation in a general circulation model. *J Geophys Res* 109:D17105. doi:10.1029/2004JD004818
- Doty B (1995) The grid analysis and display system “GrADS” V1.5.1.12. User Manual of GrADS software. <http://iges.org/grads/>. Accessed 28 November 2007
- Ernest R, Devara PCS, Shah SK, Sonbawne SM, Dani KK, Pandithuri G (2008) Temporal variations in sun photometer measured precipitation water in near IR band and comparison with model estimates at a tropical Indian station. *Atmosfera* 21:317–333
- Gaffen DJ, Robock A, Elliott WP (1992) Annual cycles of tropospheric water vapor. *J Geophys Res* 97:185–193
- Garcia JA, Serrano A, Gallego MC (2002) A spectral analysis of Iberian Peninsula monthly rainfall. *Theor Appl Climatol* 71:77–95
- Ghaiur HA, Asakereh H (2005) Fourier models application in monthly and annual temperature estimation. *Q Geogr Res* 77:83–99
- Ghaiur HA, Khosravi M (2002) ENSO effects on anomalies of summer and autumn rainfall over southeast of Iran. *Q Geogr Res* 62:141–174
- Ghaiur HA, Masudian A (1996) Investigating the changes of the total annual precipitation in Iran. *Nivar* 29:19–28
- Hadjimitsis D, Mitrika Z, Gazani I, Retalis A, Chrysoulakis N, Michaelides S (2011) Estimation of spatio-temporal distribution of precipitable water using MODIS and AVHRR data: a case study for Cyprus. *Adv Geosci* 30:23–29
- Hartmann H, Becker S, King L (2008) Quasi-periodicities in Chinese precipitation time series. *Theor Appl Climatol* 92:155–163
- Jahanbakhsh S, Edalatdust M (2008) Solar activity effects on precipitation changes in Iran. *Q Geogr Res* 88:3–24
- Kalaycı S, Karabork MC, Kahya E (2004) Analysis of El-Niño signal on Turkish streamflow and precipitation pattern using spectral analysis. *Fresenius Environ Bull* 13:719–725
- Kalnay E, Kanamitsu M, Kistler R, Collins W, Deaven D, Gandin L, Iredell M, Saha S, White G, Woollen J, Zhu Y, Leetmaa A, Reynolds R, Chelliah M, Ebisuzaki W, Higgins W, Janowiak J, Mo KC, Ropelewski C, Wang J, Jenne R, Joseph D (1996) The NCEP/NCAR 40-year reanalysis project. *Bull Am Meteorol Soc* 77:437–471
- Kerns BWJ, Chen YL, Chang MY (2010) The diurnal cycle of winds, rain, and clouds over Taiwan during the mei-yu, summer, and autumn rainfall regimes. *Mon Weather Rev* 138:497–516
- Knievel J C, Ahijevych D A, Manning KW (2004) The diurnal mode of summer rainfall across the conterminous United States in 10-km simulations by the WRF model. Preprints, 16th Conference on Numerical Weather Prediction. Am Meteorol Soc 17
- Lana MD, Martinez C, Burguen SA (2005) Periodicities and irregularities of indices describing the daily pluviometer regime of the Fabre Observatory (NE Spain) for the years 1917–1999. *Theor Appl Climatol* 82:183–198
- Lee M, Schubert SD, Suarez MJ, Held IM, Lau NC, Plushy JJ, Kumar A, Kim HK, Schema JKE (2007) An analysis of the warm-season diurnal cycle over the continental United States and northern Mexico in general circulation models. *J Hydrometeor* 8:344–366
- Mitchell JM Jr, Dzerdzeevskii B, Flohn H, Hofmeyr WL, Lamb H, Rao KN, Wallen CC (1966) Climatic Change: Technical Note No. 79, Report of Working Group of Commission for Climatology; WMO No. 195 TP 100: Geneva, Switzerland, World Meteorological Organization, 81 P
- Montazeri M (2014) Time-spatial investigation of Iran’s annual temperatures. *Geogr Dev* 36:209–228
- Nesbitt SW, Zipser EJ (2003) The diurnal cycle of rainfall and convective intensity according to three years of TRMM measurements. *J Climate* 16:1456–1475
- Niroumad HA, Bozorgnia A (2002) Introduction to the time series analysis. University of Ferdosi press, Mashhad
- Parameswaran K, Krishnamurthy BV (1990) Altitude profiles of tropospheric water vapor at low latitudes. *J Appl Meteorol* 29:665–679
- Pritchardand MS, Somerville RCJ (2009) Empirical orthogonal function analysis of the diurnal cycle of Precipitation in a multi-scale climate model. *Geophys Res Lett* 36:1–5
- Rouault M, Sen Roy S, Balling RC Jr (2012) The diurnal cycle of rainfall in South Africa in the austral summer. *Int J Climatol* 10:1–8
- Sen Roy A, Balling JRRC (2005) Harmonic and simple kriging analyses of diurnal precipitation patterns in Puerto Rico. *Caribb J Sci* 41:181–188
- Stanton ET (1968) World distribution of mean monthly and annual perceptible water. *Mon Weather Rev* 96:785–797
- Surcel M, Berenguer M, Zawadzki I (2010) The diurnal cycle of precipitation from continental radar mosaics and numerical weather

- prediction models. Part I: methodology and seasonal comparison. *Mon Weather Rev* 138:3084–3106
- Tingley MP (2012) A Bayesian ANOVA scheme for calculating climate anomalies, with applications to the instrumental temperature record. *J Climate* 25:777–791
- Twardosz R (2007) Seasonal characteristics of diurnal precipitation variation in Krakow (south Poland). *Int J Climatol* 27:957–968
- Vasic S, Lin AC, Zawadzki I, Bousquet O, Chaumont D (2007) Evaluation of precipitation from numerical weather prediction models and satellites using values retrieved from radars. *Mon Weather Rev* 135:3750–3766
- Wallace J (1975) Diurnal variations in precipitation and thunderstorm frequency over the conterminous United States. *Mon Weather Rev* 103:406–419
- Weihong Q, Lin X, Zhu Y, Xu Y, Fu J (2007) Climatic regime shift and decadal anomalous events in China. *Clim Change* 84:167–189
- Yang G, Slinger J (2001) The diurnal cycle in the tropics. *Mon Weather Rev* 129:784–801